

# Wavelet-based coherence measures of global seismic noise properties

A. A. Lyubushin

Received: 8 October 2013 / Accepted: 22 October 2014 / Published online: 29 October 2014  
© Springer Science+Business Media Dordrecht 2014

**Abstract** The coherent behavior of four parameters characterizing the global field of low-frequency (periods from 2 to 500 min) seismic noise is studied. These parameters include generalized Hurst exponent, multifractal singularity spectrum support width, the normalized entropy of variance, and kurtosis. The analysis is based on the data from 229 broadband stations of GSN, GEOSCOPE, and GEOFON networks for a 17-year period from the beginning of 1997 to the end of 2013. The entire set of stations is subdivided into eight groups, which, taken together, provide full coverage of the Earth. The daily median values of the studied noise parameters are calculated in each group. This procedure yields four 8-dimensional time series with a time step of 1 day with a length of 6209 samples in each scalar component. For each of the four 8-dimensional time series, a multiple correlation measure is estimated, which is based on computing robust canonical correlations for the Haar wavelet coefficients at the first detail level within a moving time window of the length 365 days. These correlation measures for each noise property demonstrate essential increasing starting from 2007 to 2008 which was continued till the end of 2013. Taking into account a well-known phenomenon of noise correlation increasing before catastrophes, this increasing of seismic noise synchronization is interpreted as indicators of the strongest (magnitudes not less than 8.5)

earthquakes activation which is observed starting from the Sumatra mega-earthquake of 26 Dec 2004. This synchronization continues growing up to the end of the studied period (2013), which can be interpreted as a probable precursor of the further increase in the intensity of the strongest earthquakes all over the world.

**Keywords** Global low-frequency seismic noise · Synchronization · Multifractals · Normalized entropy of variance · Kurtosis · Wavelet-based robust canonical correlations · Global seismic activity

## 1 Introduction

Microseismic oscillations in a wide frequency range are one of the most frequently investigated topics of geophysical studies. This is due to their accessibility, the presence of numerous regional and global seismic networks, and the well-developed practice of seismic observations. Even an approximate review of the literature devoted to analysis of microseisms apparently cannot be made. This is particularly true of the analysis of high frequency (HF) microseisms (from 0.01 to 100 Hz and higher, up to seismoacoustic waves). The widespread occurrence of HF microseismic observations is due to the relative simplicity and mobility of instrumentation free from rigid requirements on long-term stability of sensors that can by no means be neglected in problems of low-frequency (LF) geophysical monitoring. In the paper (McNamara and Buland (2004)), the results were presented of detailed research into microseismic

A. A. Lyubushin (✉)  
Institute of Physics of the Earth, Russian Academy of Sciences, Moscow,  
B. Gruzinskaya, 10, Moscow, Russia 123995  
e-mail: lyubushin@yandex.ru

background of natural and industrial origin in the frequency band 0.01–16 Hz, including the construction of estimators for the temporal (diurnal and seasonal) and spatial distribution of power spectrum properties. More recent studies on the composition of short-period microseisms are presented in Koper and de Foy (2008) and Koper et al. (2010). With an increase in the period of microseismic background oscillations studied, the role of atmospheric and oceanic waves as main sources of microseisms becomes predominant. Berger et al. (2004) presented a review of the use of IRIS broadband seismic stations for the study of background microseisms. Microseismic oscillations in the period range 5–40 s were studied by Stehly et al. (2006), who established their oceanic origin. Continuously observed microseismic oscillations at periods of 100–500 s were examined in Friedrich et al. (1998), Kobayashi and Nishida (1998), Tanimoto (2001, 2005), and Arduin et al. (2011). These oscillations are generated both by weak earthquakes and by processes in the atmosphere and ocean. In the papers Aster et al. (2008), Grevemeyer et al. (2000), Kedar et al. (2008), and Schimmel et al. (2011), variability of field of microseisms due to climate change and ocean processes were studied.

In order for earthquakes to be a source of continuously present microseismic oscillations, at least one earthquake with a magnitude of 6 should occur daily to maintain the observed intensity of such oscillations. The cumulative effect of all weak earthquakes estimated from the Gutenberg–Richter recurrence law yields an energy contribution one to two orders smaller than the observed value. The effect of atmospheric processes (movement of cyclones) and oceanic waves generated by them, as well as the impact of the waves on the shelf and coasts, contributes most to the energy of the low-frequency (LF) microseismic background. The origin of an LF seismic hum with a predominant period of 4 min was studied in Rhie and Romanowicz (2004, 2006). A significant correlation was established between the intensity of these oscillations and the storm wave height in the oceans, and it was shown that the hum intensity is independent of the Earth's seismic activity: the authors presented an example of a seismically quiet time interval (January 31–February 3, 2000) characterized, however, by anomalously high amplitudes of microseismic background in the vicinity of the 4-min period. As a possible mechanism of excitation of such oscillations, they proposed the perturbation of the gravitational field by high waves resulting in the excitation of LF seismic waves on the seafloor. The main regions of excitation of these

oscillations are suggested to be the North Pacific Ocean in winter and the southern Atlantic Ocean in summer. This frequency range of the ambient seismic noise (“seismic hum”) was investigated in Fukao et al. (2010) and Nishida et al. (2008, 2009).

An important trend in analyzing seismic noise is used for tomography (Shapiro et al. 2005, 2006; Bonnefoy-Claudet et al. 2006; Yang and Ritzwoller 2008; Bensen et al. 2007; Lawrence and Prieto 2011). The main tool of using ambient seismic noise for tomography is estimating cross-correlation function between rather long records of seismic noise at different stations. A similar approach was used in Campillo and Paul (2003a, b) and Campillo (2006) for investigating coda. Ambient seismic noise tomography based on using body waves generated mainly by ocean wind, storms, and cyclones were studied in Landes et al. (2010), Poli et al. (2012), Zhang et al. (2009), and Zhang et al. (2010a, b). In the papers Brenguier et al. (2008, 2011), analysis of seismic noise applies to monitoring of volcanic activity.

The main difference in the study in this paper is that we use correlations and coherence effects not for initial seismic records but in time series of their properties estimated within adjacent time windows. Besides that, our purpose is investigating of variability of seismic noise properties coherence in much lower-frequency range—up to periods of several days.

In spite of the fact that the main source of energy for LF microseisms is an external one with respect to the Earth's crust, and the latter is merely the propagation medium, the conditions in the Earth's crust affect the statistical characteristics and the specific features in the behavior of LF microseismic vibrations. Consequently, if we study the time variations of the characteristics of seismic noise, this study will hopefully yield important information concerning the changes in the Earth's crust, including those linked with the seismic process and with the preparation of strong earthquakes.

This basically simple idea of the use of low-frequency microseismic oscillations for monitoring the lithosphere, nevertheless, cannot be realized in a simple way. The main difficulty consists in a strong influence of numerous uncorrelated sources of the data. These sources are often diffusely distributed over the Earth's surface. Therefore, it is impossible in this case to investigate the transmitting properties of the lithosphere by controlling input actions and responses. Additionally, the division into “a signal” and “noise,” which is typical of the traditional methods used for data analysis, loses

its sense, when microseismic oscillations are processed. Only tidal variations in the amplitude of microseisms, as well as the arrivals and coda from the well-known strong earthquakes, can be related to “signals.” These signals have been long and traditionally used in geophysics. All other microseism variations relate to “noise.”

In this paper, the main tool for overcoming the influence of uncorrelated random sources is using different statistics (properties of noise waveforms) calculated within adjacent “short” time fragments. Thus, seismic noise records are transformed into time series with “big” sampling time step, 1 day for instance. These time series are much more correlated and are more suitable for investigating of synchronization effects.

This paper is a continuation of a series of papers (Lyubushin 2008–2014) which were devoted to the analysis of different statistics obtained from LF seismic noise waveforms (mainly multifractal properties) for the problems of earthquakes predictions. The main purpose of the paper is investigating of effects of synchronization of the variations of different properties of global LF seismic noise.

During the previous 10 years, a strong increase of seismic activities of the Earth is observed: among the 17 strongest earthquakes (with magnitude not less than 8.5), six events took place starting from the Sumatra mega-earthquake of 26 Dec 2004. The main result of the paper is the following: the increasing of strongest earthquake intensity correlates with the increasing of synchronization effects of global LF seismic noise properties. The increasing of seismic noise synchronization observed till now is what could be a precursor of occurrence of strong earthquakes in the near future.

## 2 Data

The seismic records were taken by requests to IRIS database by the address <http://www.iris.edu/forms/webrequest/> from 229 seismic stations of three global broadband seismic networks:

Global Seismographic Network: [http://www.iris.edu/mda/\\_GSN](http://www.iris.edu/mda/_GSN)  
 GEOSCOPE: <http://www.iris.edu/mda/G>  
 GEOFON: <http://www.iris.edu/mda/GE>

Vertical components with sampling rate 1 Hz (LHZ-records) were downloaded for 16 years of observation since 01 Jan. 1997 up to 31 Dec. 2013. The initial LHZ-

records were transformed to sampling time step 1 min by calculating mean values within successive time intervals of the length 60 s. A further analysis is based on estimating statistical properties of low-frequency seismic noise waveforms (periods exceeding 2 min) within successive daily time intervals of the length 1440 samples with time step 1 min.

Figure 1 presents positions of 229 broadband seismic stations all over the world and their splitting into eight groups of stations. Each group has a three letter identification code, and the number of stations within each group is given in brackets. The names of the groups have the following abbreviation sense: the first letter is “N” or “S” which means North or South. The second letter is “E” or “W” which means East or West. Thus, initially, all station were divided into four parts by splitting into Northeast, Northwest, Southeast, and Southwest quarter-spheres. Finally, each of the four parts was split into the North and South parts (the third letter is “N” or “S”) by the rule that the number of stations within each part must be approximately equal to each other.

## 3 Description of seismic noise waveforms statistics

The seismic records from each station after coming to 1 min sampling time step were split into adjacent time fragments of the length of 1 day (1440 samples) and for each fragment four parameters of low-frequency daily seismic noise waveforms were calculated. Two of them are multifractal parameters: generalized Hurst exponent  $\alpha^*$  and singularity spectrum support width  $\Delta\alpha$ . Two other seismic noise parameters are kurtosis  $\kappa$  and normalized entropy of variance EntVar. Thus, the time series of  $\alpha^*$ ,  $\Delta\alpha$ ,  $\kappa$ , and EntVar values with sampling time step 1 day were obtained from each of the 229 seismic stations which are presented at Fig. 1. Figure 2 illustrates the sequence of data transform operations.

Estimates of multifractal properties  $\alpha^*$  and  $\Delta\alpha$  of low-frequency seismic noise were used in the paper Lyubushin (2008–2014) for the purposes of earthquake prediction and dynamic estimate of seismic danger. The normalized entropy of seismic noise variance EntVar was introduced in Lyubushin (2014). A brief description of the used statistics is given below.

Multifractal singularity spectrum  $F(\alpha)$  of the signal  $X(t)$  is defined as a fractal dimensionality of time moments  $t_\alpha$  which have the same value of the local

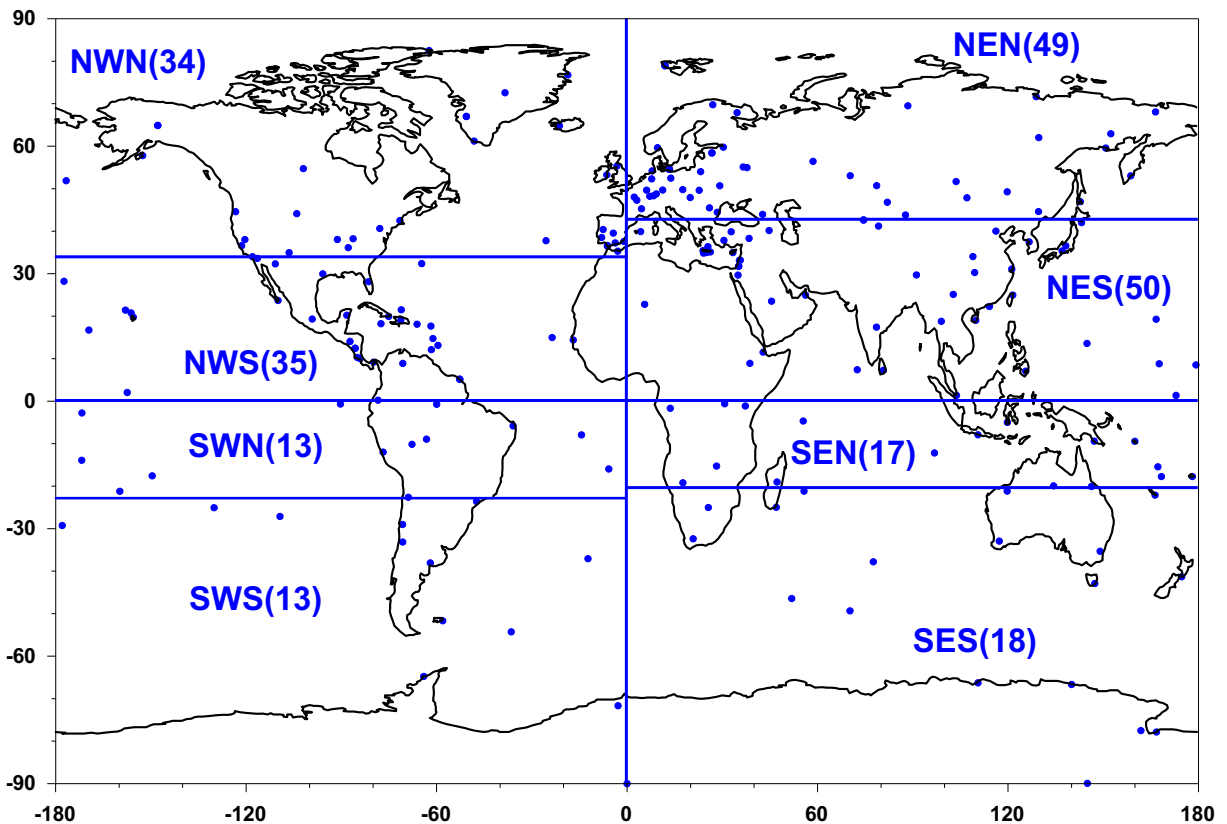


**Fig. 1** Positions of 229 broadband seismic stations and their splitting into eight groups with number of stations in each group in brackets

Lipschitz-Holder exponent  $h(t) = \lim_{\delta \rightarrow 0} \frac{\ln(\mu(t, \delta))}{\ln(\delta)}$ , i.e.,  $h(t_\alpha) = \alpha$ , where  $y$  is a measure of signal variability in the vicinity of time moment  $t$  (Feder 1988). If  $X(t)$  is a usual self-similar monofractal signal with Hurst exponent value  $0 < H < 1$  (Taqqu 1988), then  $F(H) = 1, F(\alpha) = 0 \forall \alpha \neq H$  but finite sample estimate of singularity spectrum does not obey these rigorous theoretical conditions of course.

Practically the most convenient method for estimating singularity spectrum is a multifractal detrended fluctuation analysis (DFA) (Kantelhardt et al. 2002) which is used here. The function  $F(\alpha)$  could be characterized by the following parameters:  $\alpha_{\min}, \alpha_{\max}, \Delta\alpha = \alpha_{\max} - \alpha_{\min}$  and  $\alpha^*$ —an argument providing maximum to singularity spectra:  $F(\alpha^*) = \max_{\alpha} F(\alpha)$ . Parameter  $\alpha^*$  is called a generalized Hurst exponent, and it gives the most typical value of the Lipschitz-Holder exponent. Parameter  $\Delta\alpha$ , singularity spectrum support width, could be regarded as a measure of variety of stochastic behavior. It should be noticed that usually  $F(\alpha^*) = 1$ —maximum of singularity spectra equals to the dimensionality of the embedding set, i.e., to dimensionality of

time interval. For removing scale-dependent trends (which are mostly caused by tidal variations) in multifractal DFA-method of singularity spectrums estimates, a local polynomial of the eighth order was used.

Figure 3 illustrates the notion of singularity spectrum. Spectral analysis traditionally used in the geophysical practice does not provide an insight of the structure of low-frequency seismic noise and in other geophysical monitoring signals because often these signals do not contain either monochromatic components or narrow-band signals. That is why multifractal analysis becomes more and more popular in geophysical studies (Ramirez-Rojas et al. 2004; Ida et al. 2005; Currenti et al. 2005; Telesca et al. 2005; Lyubushin 2009, 2010, 2011a, b, 2012, 2013a, b, 2014; Lyubushin et al. 2013, 2014).

Kurtosis  $\kappa$  is defined by the formula (Cramer 1999):

$$\kappa = \frac{\langle (\Delta x)^4 \rangle}{\langle (\Delta x)^2 \rangle^2} - 3 \quad (1)$$

Here,  $\Delta x$  is deflection of the daily noise waveform from trend which is chosen as polynomial of the eighth

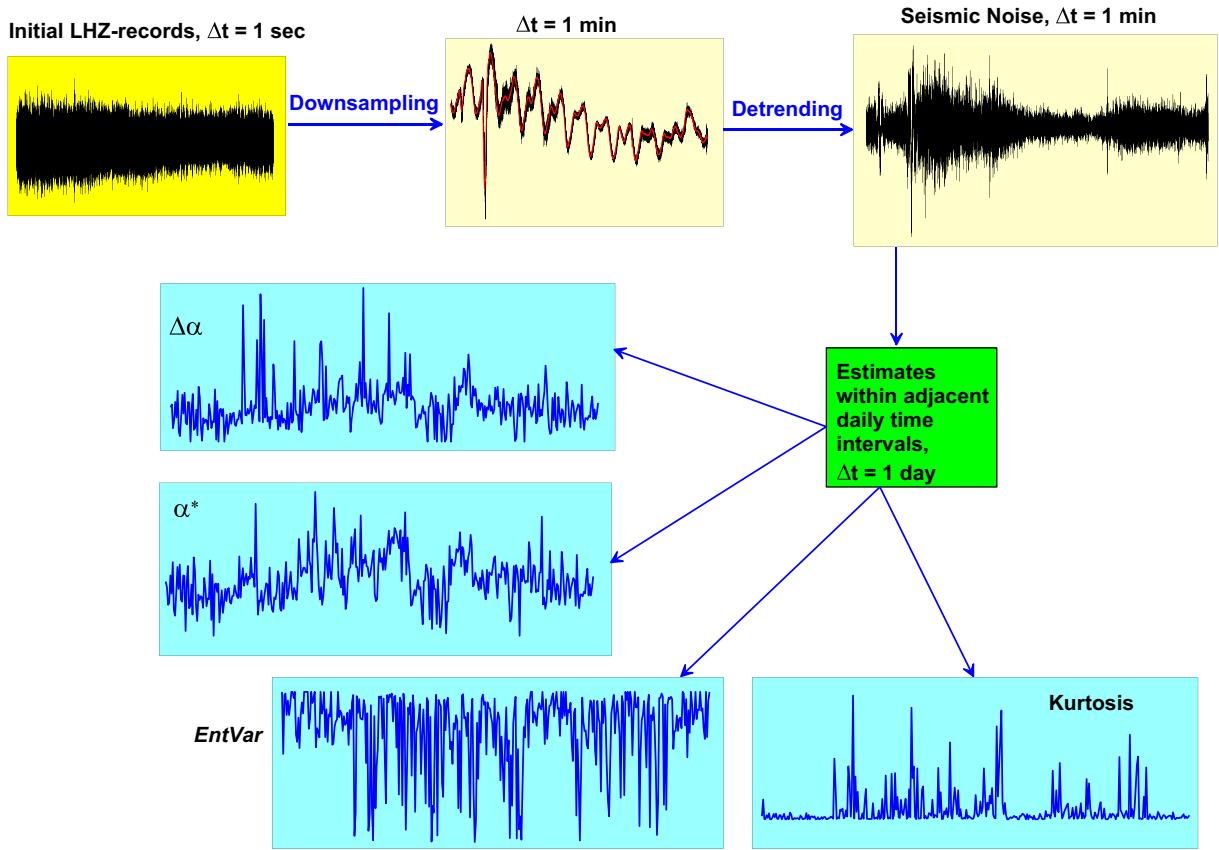
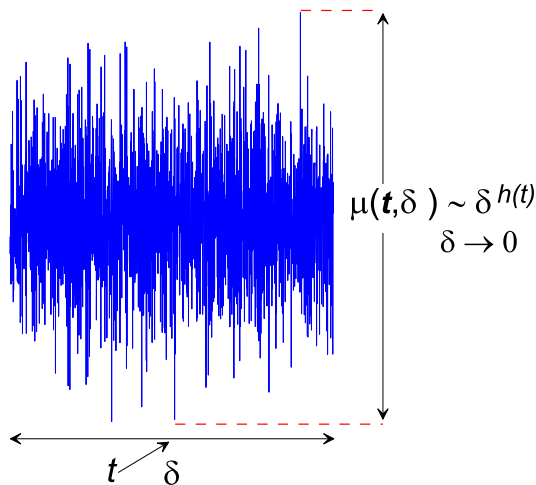


Fig. 2 Scheme of data transform

order,  $\langle \dots \rangle$  is the symbol of sample estimate of mean value. Kurtosis characterizes the sharpness of

probability distribution form and gives a measure of deflection of  $\Delta x$  from normal distribution for which

**Measure of the random signal variability at the time interval  $[t - \delta/2, t + \delta/2]$**



**Multi-fractal singularity spectrum  $F(\alpha)$  and its parameters:  $\Delta\alpha$  - support width and  $\alpha^*$  - generalized Hurst exponent.**

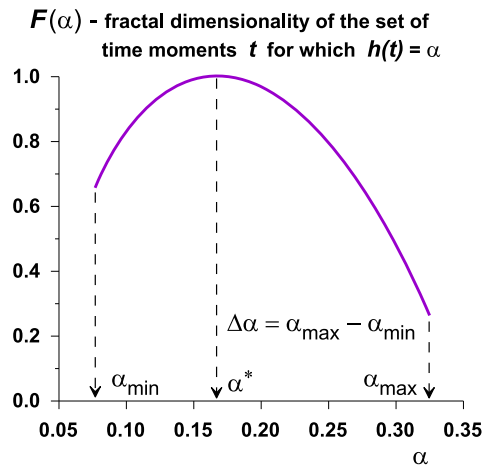


Fig. 3 Multi-fractal singularity spectrum and its parameters

$\kappa=0$ . If  $\kappa \gg 1$ , then signal is called leptokurtotic and this property means the existence of “fatter tails” of distribution. The seismic noise is leptokurtotic.

Let us introduce normalized entropy of variance (Lyubushin 2014). For this purpose, let us split each daily noise waveform into 24 parts which correspond to adjacent hour intervals. Let  $V_\alpha, \alpha=1, \dots, m_V=24$  be variance values which are calculated for increments of waveforms (after removing tidal trends from daily waveforms) within adjacent time intervals of the length 60 samples, i.e., for adjacent hour time intervals. After that, let us calculate the normalized entropy of variance distribution by the formula:

$$\begin{aligned} \text{EntVar} &= -\sum_{\alpha=1}^{m_V} p_\alpha \cdot \log(p_\alpha) / \log(m_V), p_\alpha \\ &= V_\alpha / \sum_{\beta=1}^{m_V} V_\beta, 0 \leq \text{EntVar} \leq 1 \end{aligned} \tag{2}$$

#### 4 Results of seismic noise properties estimating

Figure 4 presents 16 graphics of median values of 4 statistics  $\alpha^*$ ,  $\Delta\alpha$ ,  $\kappa$ , and EntVar calculated each day for 17 years (1997–2013, 6209 daily samples in each scalar time series) from 8 groups of stations which are presented at Fig. 1. It is interesting to notice that variations of all noise parameters for two groups, NWN and NEN, have the most explicit annual periodic components. The next step consists of estimating of evolution of some multi-dimensional measure of correlation between variations of 8-dimensional time series of each LF seismic noise properties in a moving time window.

#### 5 Wavelet-based multiple correlations

Let  $u_r(t), r=1, \dots, m, t=1, \dots, N$  be a sequence of Haar wavelet (Mallat 1998) coefficients for the first detail level of multiple time series,  $t$  is time index. Let us present the  $p$ -th component of Haar wavelet coefficients time series as a sum:

$$\begin{aligned} u_p(t) &= w_p(t) + \varepsilon_p(t), w_p(t) \\ &= \sum_{r=1, r \neq p}^N \gamma_r^{(p)} \cdot u_r(t), 1 \leq p \leq m \end{aligned} \tag{3}$$

Coefficients  $\gamma_r^{(p)}$  are found from the problem of minimum of sum of absolute values (which provides robustness of estimate):

$$\begin{aligned} \gamma_r^{(p)} &: \sum_{t=1}^N |\varepsilon_p(t)| \\ &= \sum_{t=1}^N \left| u_p(t) - \sum_{r=1, r \neq p}^N \gamma_r^{(p)} \cdot u_r(t) \right| \rightarrow \min_{\gamma_r^{(p)}} \end{aligned} \tag{4}$$

Robust canonical correlation  $\rho_p$  of  $p$ -th component is defined as robust correlation coefficient (Huber and Ronchetti 2009) between  $u_p(t)$  and  $w_p(t)$ :

$$\begin{aligned} \rho_p &= \frac{S(\varphi_p^2) - S(\psi_p^2)}{S(\varphi_p^2) + S(\psi_p^2)}, \varphi_p(t) \\ &= \frac{u_p}{S(u_p)} + \frac{w_p}{S(w_p)}, \psi_p(t) = \frac{u_p}{S(u_p)} - \frac{w_p}{S(w_p)} \end{aligned} \tag{5}$$

where  $S(\xi) = \text{med}|\xi - \text{med}(\xi)|$ ,  $\text{med}(\xi)$  is median of the value  $\xi$ , and  $S(\xi)$  is an absolute median deviation of the value  $\xi$ .

The value (5) is called robust canonical correlation because if the problem (4) would be substituted for usual least squares minimization problem and correlation coefficient in the formula (5) would be calculated by the classic formula

$\rho_p = \text{cov}(u_p, w_p) / \sqrt{\text{cov}(u_p, u_p) \cdot \text{cov}(w_p, w_p)}$ , then  $\rho_p$  would be canonical correlation (Hotelling 1936; Rao 1965) of the scalar variable  $u_p(t)$  with respect to  $(m-1)$ -dimensional vector of all other components of vector  $u(t)$ . The need to replace the classic scheme of the calculation of canonical correlations by its robust variant is dictated by the strong instability of the result of the classic calculations with respect to outliers in wavelet coefficients (see Fig. 5). We should emphasize that the method is robust in two procedures: the solution of minimization problem (4) by the method of least moduli rather than by least squares and the calculation of the correlation coefficient by formula (5).

Multiple correlation coefficient  $\mu$  is defined as the product of absolute values of all canonical correlations  $\rho_p$ :

$$\mu = \prod_{p=1}^m |\rho_p|, 0 \leq \mu \leq 1 \tag{6}$$

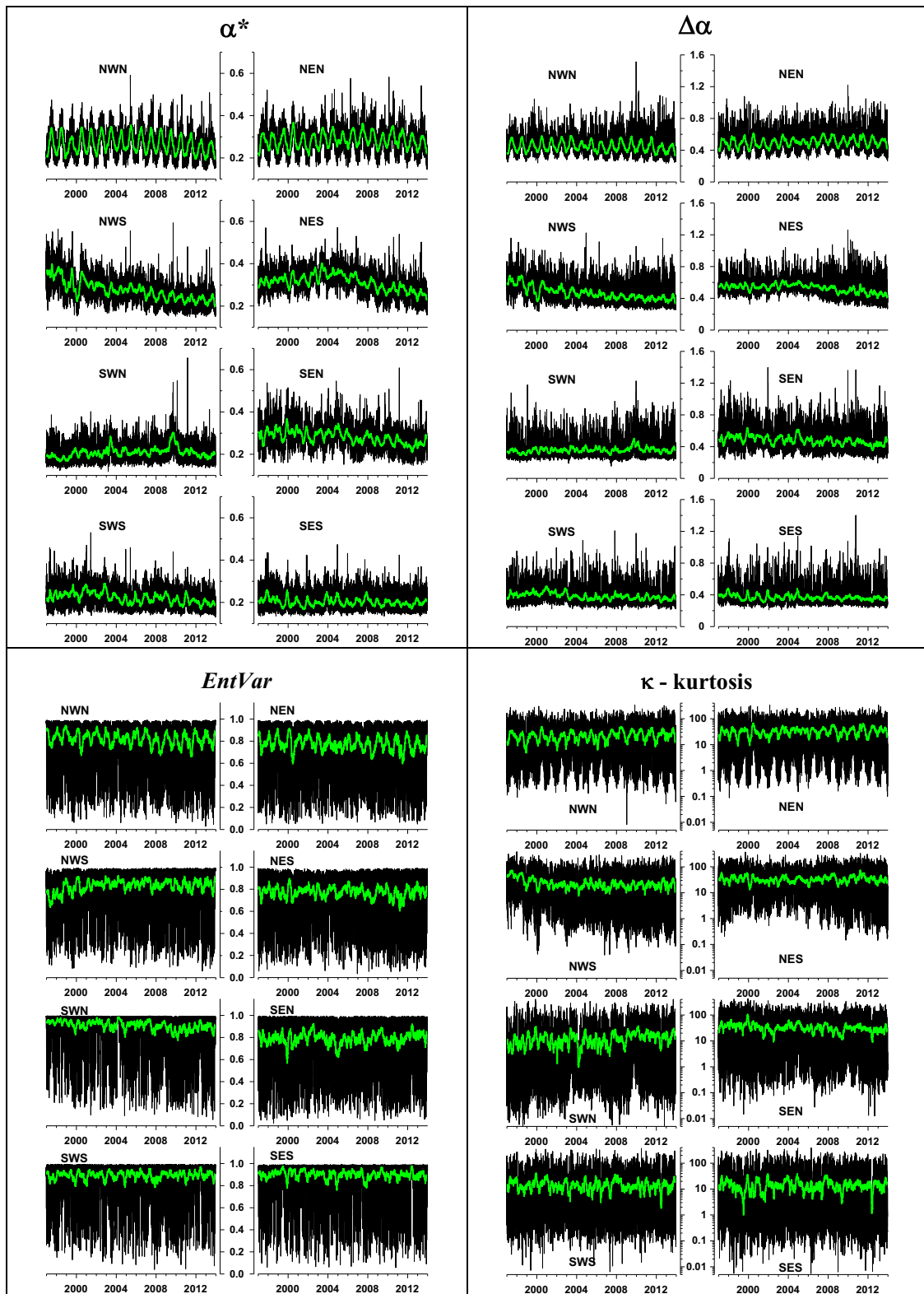


**Fig. 4** Daily median values of the four parameters of low-frequency seismic noise from the eight groups of stations presented at Fig. 1. *Bold green lines* are graphics of running average within moving time window of the length 57 days

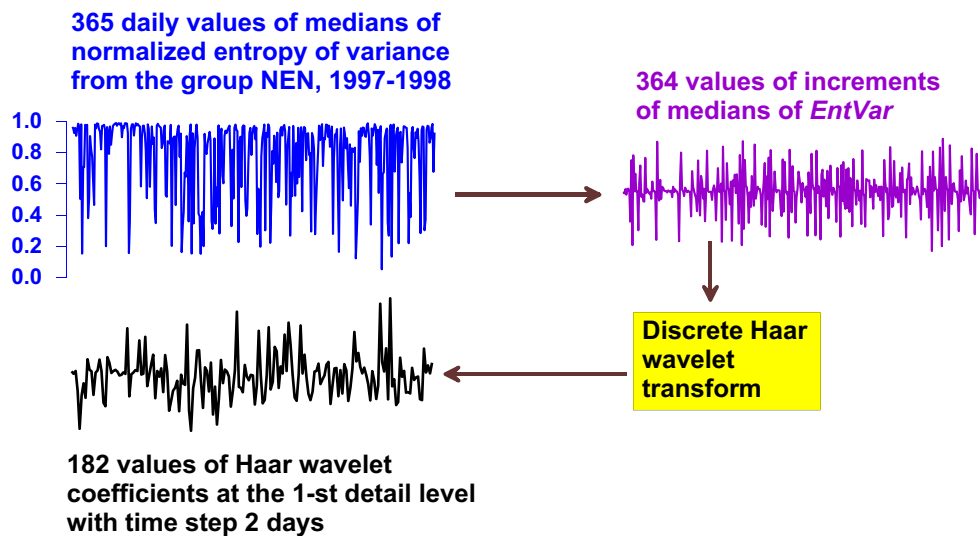


**Fig. 5** Example of getting Haar wavelet coefficients from one group of stations for further estimating of multiple correlations within time window of the length 365 days

If the value (6) will be calculated within moving time window of the certain length, then the value (6) will be dependent on the time position  $\tau$  of the right-hand end of moving time window:  $\mu = \mu(\tau)$ . The values of multiple correlation measure (6) range from 0 to 1. Let  $\Delta t$  be the time step of multidimensional time series to be analyzed, in our case  $\Delta t = 1$  day. The larger the value of (6), the stronger the overall connection between all analyzed processes on time scales between  $2\Delta t$  and  $4\Delta t$ . This range corresponds to the first detail level of orthogonal wavelet decomposition (Mallat 1998). We should emphasize that the value of (6) is the product of  $m$  non-negative values with moduli less than unity. Therefore, the greater the number  $m$  of the series analyzed, the lower the absolute values of  $\mu(\tau)$ . As a consequence, the absolute values of statistic (6) can be compared only for the same number of series  $m$ . Most interesting are not the absolute values of measure (6) but its relative values for different values of  $\tau$ .

Haar wavelets are chosen with a purpose to detect the most abrupt synchronous changes of seismic noise properties. The length of time window was taken for 365 days—this choice is quite natural taking into account the annual periodicity of noise properties (see Fig. 4). Using of annual time window provides excluding seasonal variations of synchronization effects. It is possible to calculate measure (6) not for the first detail level only but for other levels as well. This would make the measure (6) level-dependent which is similar to frequency-dependent statistics in multidimensional

spectral analysis. We decided to restrict ourselves by first detail level only because such analysis has the goal of detecting the quickest changes of the noise field properties. Besides that reason, it should be noticed that the number of wavelet coefficients decreases twice with increase in the number of detail level on one. It means that estimates for the first detail level are the most statistically significant because the number of wavelet coefficients at the first detail level equals half of the number of samples within the time window and is the maximum. Thus,  $N = 182$  in the formulas (3–4). The Haar wavelet transforms were applied to seismic noise properties variations after coming to their increments. All stages of getting Haar wavelet coefficients for further use for calculating multiple correlation coefficients are illustrated at the Fig. 5.

Figure 6 presents graphics of statistics  $\mu(\tau)$  for each of four 8-dimensional time series in dependence on the position  $\tau$  of the right-hand end of the annual moving time window with their trends fitted by polynomials of the third order.

## 6 Discussion and conclusion

Study of the characteristics of noise in complex systems is one of the most promising directions of scientific research. This is a consequence of a general trend in studying processes in complex non-linear systems in physics, biology, finances, and other fields where

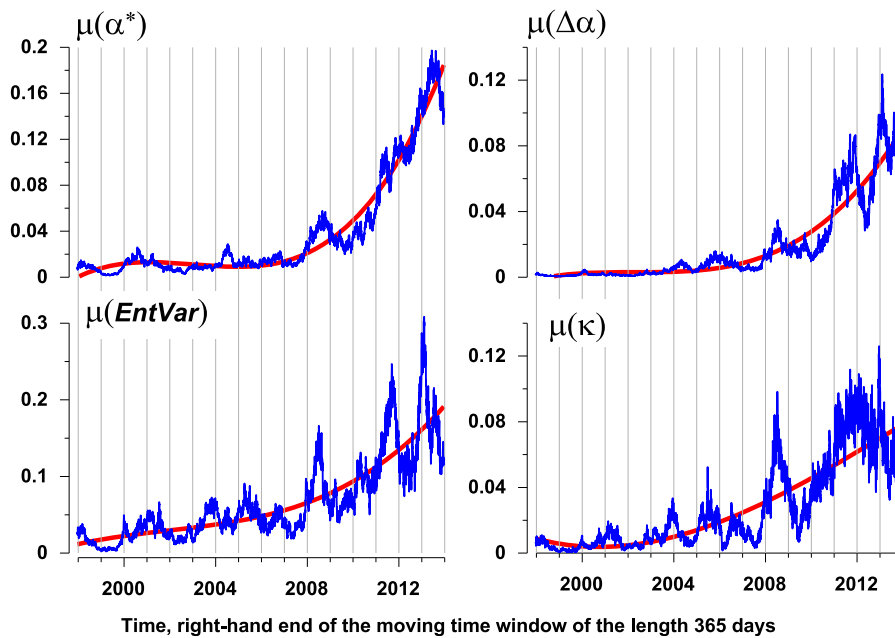


**Fig. 6** Graphics of wavelet-based robust multiple correlations for the first detail level of 8-dimensional time series presented at Fig. 4. *Bold red lines* present polynomial trends of third order

ambient noise is regarded as an important source of information. Such studies lie on the borderline of different disciplines since there is much more similarity in this field than the differences associated with the individual properties of the studied objects. In this sense, the study of such a complex system as the Earth constitutes no exception. The low-frequency seismic noise caused by the interaction between the lithosphere, atmosphere, and ocean has a complicated statistical structure, which contains the information about the preparation of the geological catastrophes including large earthquakes.

In this paper, the analysis covers the data from a large number of broadband seismic stations globally distributed all over the world with the aim to identify the variability of global effects of synchronization in seismic noise in a moving time window. It is known that, starting from the mega-earthquake in Sumatra on 26 Dec. 2004, the Earth experienced a series of the strongest earthquakes ( $M \geq 8.5$ ), which have not occurred since the beginning of 1965. This information is presented in the Table 1. We can notice that among these 17 strongest seismic events, 6 took place during the last 10 years. During the previous time interval of 40 year duration, 1965–2004, no strongest events took place at all. Moreover, among these six strongest earthquakes, four occurred during the last 7 years, since 2007. Thus,

the last 10 years are marked by the significant increasing of seismic intensity with acceleration.

The following questions now arise: how is this activation reflected in the coherence of time series of the parameters characterizing the global seismic noise? From graphics of evolution of multiple correlations  $\mu(\tau)$  at Fig. 6, it is evident that starting from the annual time window corresponding to 2007 (with right-hand time mark 2008), an increasing of synchronization is observed for all properties of seismic noise.

In the theory of complex systems, a phenomenon of increasing radius of correlations of statistical fluctuations (i.e., ambient noise of the system), “critical opalescence” in the theory of phase transitions, is a well-known indicator of approaching to abrupt changes of the system, to catastrophe (Gilmore 1981; Nicolis and Prigogine 1989).

The purpose of this paper is not an earthquake prediction in some certain place. We took rather arbitrary four dimensionless parameters of very low-frequency seismic noise and studied their multiple correlations from eight different parts of the world. It turns out that the correlations are increasing in time, and this increasing coincides with dramatic increasing of strongest earthquakes rate which is observed starting from the Sumatra mega-earthquake at 26 Dec of 2004, especially

**Table 1** Strongest earthquakes,  $M \geq 8.5$ , from the beginning of the twentieth century

Date	Magnitude	Latitude	Longitude	Date	Magnitude	Latitude	Longitude
1906.01.31	8.8	1	-81.5	1964.03.28	9.2	61.02	-147.65
1922.11.11	8.5	-28.55	-70.5	1965.02.04	8.7	51.21	178.5
1923.02.03	8.5	54	161	2004.12.26	9.1	3.3	95.78
1938.02.01	8.5	-5.05	131.62	2005.03.28	8.6	2.08	97.01
1950.08.15	8.6	28.5	96.5	2007.09.12	8.5	-4.438	101.367
1952.11.04	9.0	52.76	160.06	2010.02.27	8.8	-35.846	-72.719
1957.03.09	8.6	51.56	-175.39	2011.03.11	9.0	38.322	142.369
1960.05.22	9.5	-38.29	-73.05	2012.04.11	8.6	2.311	93.063
1963.10.13	8.5	44.9	149.6				

Source: [http://earthquake.usgs.gov/earthquakes/world/10\\_largest\\_world.php](http://earthquake.usgs.gov/earthquakes/world/10_largest_world.php)

starting from 2007. Taking into account that we investigated a range of periods from 2 min up to 500 min, this correlation increasing could not be the direct consequence of aftershocks of strongest earthquakes. Our hypothesis is that slow movements of small Earth's crust blocks are synchronized in the regions of preparing huge earthquakes (Lyubushin 2009, 2010, 2011a, b, 2012, 2013a, b) and we see that this synchronization is a global phenomenon starting from the beginning of 2000s. Thus, we propose that we should wait for a series of strongest earthquakes in the near future.

We used the moving time window of the length 365 days, i.e., 1 year. This length seems to be the most natural because of evident seasonal variations of seismic noise properties which are presented at Fig. 4. For this reason, this length is minimal for extracting multiple correlations because of the lengths which are less than 1-year; correlations will be modulated by seasonal effects. At the same time, it is possible to test the lengths which are more than 1 year. In Fig. 7, the values of multiple wavelet-based correlations (6) are presented for two lengths of time window: 2 and 3 years. We see that

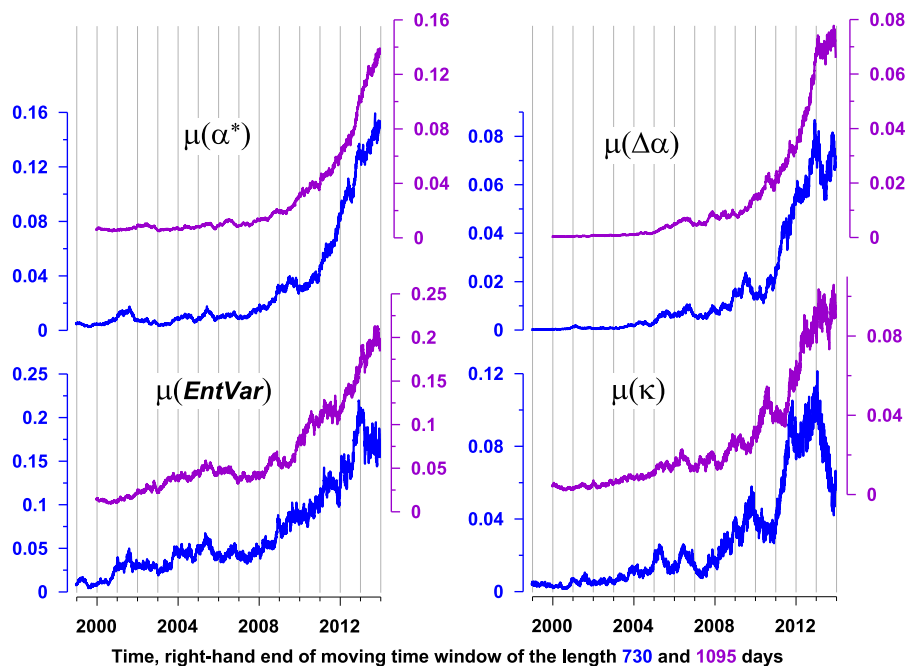


**Fig. 7** Graphics of wavelet-based robust multiple correlations for the first detail level of 8-dimensional time series presented at Fig. 4 for two lengths of moving time window: *blue lines* for the length 730 days (2 years), *purple lines* for the length 1095 days (3 years)

for the length of 3 years, multiple correlations are increasing with the explicit monotonous trend for all properties of seismic noise. The same is for the length of 2 years except the courtesies which has a non-monotonous peculiarity at the end interval of observations.

**Acknowledgments** The work was financially supported by the Russian Foundation for Basic Research (project no. 12-05-00146) and the Ministry of Education and Science of the Russian Federation (in accordance with the requirements of the contract No. 14.577.21.0109)

## References

- Ardhuin F, Stutzmann E, Schimmel M, Mangeney A (2011) Ocean wave sources of seismic noise. *J Geophys Res* 116: C09004
- Aster R, McNamara D, Bromirski P (2008) Multidecadal climate induced variability in microseisms. *Seismol Res Lett* 79:194–202
- Bensen GD, Ritzwoller MH, Barmin MP, Levshin AL, Lin F, Moschetti MP, Shapiro NM, Yang Y (2007) Processing seismic ambient noise data to obtain reliable broad-band surface wave dispersion measurements. *Geophys J Int* 169:1239–1260
- Berger J, Davis P, Ekstrom G (2004) Ambient earth noise: a survey of the Global Seismographic Network. *J Geophys Res* 109: B11307
- Bonnefoy-Claudet S, Cotton F, Bard P-Y (2006) The nature of noise wavefield and its applications for site effects studies: a literature review. *Earth Sci Rev* 79:205
- Brenguier F, Shapiro N, Campillo M, Ferrazzini V, Duputel Z, Coutant O, Nercessian A (2008) Toward forecasting volcanic eruption using seismic noise. *Nat Geosci* 1:126–130
- Brenguier F, Clarke D, Aoki Y, Shapiro NM, Campillo M, Ferrazzini V (2011) Monitoring volcanoes using seismic noise correlations. *Compt Rendus Geosci* 343:633–638
- Campillo M (2006) Phase and correlation in “Random” seismic fields and the reconstruction of the green function. *Pure Appl Geophys* 163:475–502
- Campillo M, Paul A (2003a) Long-range correlations in the diffuse seismic coda. *Science* 299(5606):547–549
- Campillo M, Paul A (2003b) Long-range correlations in the seismic coda. *Science* 299:547–549
- Cramer H (1999) *Mathematical methods of statistics*. Princeton University Press, 575 pp
- Currenti G, del Negro C, Lapenna V, Telesca L (2005) Multifractality in local geomagnetic field at Etna volcano, Sicily (southern Italy). *Nat Hazards Earth Syst Sci* 5:555–559
- Feder J (1988) *Fractals*. Plenum Press, New York
- Friedrich A, Krüger F, Klinge K (1998) Ocean-generated microseismic noise located with the Gräfenberg array. *J Seismol* 2(1):47–64
- Fukao YK, Nishida K, Kobayashi N (2010) Seafloor topography, ocean infragravity waves, and background love and Rayleigh waves. *J Geophys Res* 115:B04302
- Gilmore R (1981) *Catastrophe theory for scientists and engineers*. Wiley, New York
- Grevemeyer I, Herber R, Essen H-H (2000) Microseismological evidence for a changing wave climate in the northeast Atlantic Ocean. *Nature* 408:349–352
- Hotelling H (1936) Relations between two sets of variates. *Biometrika* 28:321–377
- Huber PJ, Ronchetti EM (2009) *Robust statistics*, 2nd Edition. John Wiley & Sons, Inc. 354 p. doi:10.1002/9780470434697.ch1
- Ida Y, Hayakawa M, Adalev A, Gotoh K (2005) Multifractal analysis for the ULF geomagnetic data during the 1993 Guam earthquake. *Nonlinear Process Geophys* 12:157–162
- Kantelhardt JW, Zschiegner SA, Konsciency-Bunde E, Havlin S, Bunde A, Stanley HE (2002) Multifractal detrended fluctuation analysis of nonstationary time series. *Phys A* 316:87–114
- Kedar S, Longuet-Higgins M, Webb F, Graham N, Clayton R, Jones C (2008) The origin of deep ocean microseisms in the North Atlantic Ocean. *Proc R Soc A* 464:777–793
- Kobayashi N, Nishida K (1998) Continuous excitation of planetary free oscillations by atmospheric disturbances. *Nature* 395:357–360
- Koper KD, de Foy B (2008) Seasonal anisotropy in short-period seismic noise recorded in South Asia. *Bull Seismol Soc Am* 98:3033–3045
- Koper KD, Seats K, Benz H (2010) On the composition of earth’s short-period seismic noise field. *Bull Seismol Soc Am* 100(2):606–617, April 2010
- Landes M, Hubans F, Shapiro N, Paul A, Campillo M (2010) Origin of deep ocean microseisms by using teleseismic body waves. *J Geophys Res* 115:B05302
- Lawrence JF, Prieto GA (2011) Attenuation tomography of the western united states from ambient seismic noise. *J Geophys Res* 116:B06302
- Lyubushin AA (2008) Microseismic noise in the low frequency range (periods of 1–300 min): properties and possible prognostic features. *Izv Phys Solid Earth* 44(4):275–290
- Lyubushin AA (2009) Synchronization trends and rhythms of multifractal parameters of the field of low-frequency microseisms—Izvestiya. *Phys Solid Earth* 45(5):381–394
- Lyubushin A (2010) Multifractal parameters of low-frequency microseisms // V. de Rubeis et al. (eds.) *Synchronization and triggering: from fracture to earthquake processes*, GeoPlanet: Earth Planet Sci 1, doi:10.1007/978-3-642-12300-9\_15, Springer-Verlag Berlin Heidelberg 2010, 388p., Chapter 15, 253–272
- Lyubushin AA (2011a) Cluster analysis of low-frequency microseismic noise—Izvestiya. *Phys Solid Earth* 47(6):488–495
- Lyubushin AA (2011b) Seismic catastrophe in Japan on March 11, 2011: long-term prediction on the basis of low-frequency microseisms—Izvestiya. *Atmos Ocean Phys* 46(8):904–921
- Lyubushin A (2012) Prognostic properties of low-frequency seismic noise. *Nat Sci* 4(8A):659–666. doi:10.4236/ns.2012.428087
- Lyubushin AA (2013a) Mapping the properties of low-frequency microseisms for seismic hazard assessment. *Izv Phys Solid Earth* 49(1):9–18. doi:10.1134/S1069351313010084

- Lyubushin A (2013b) How soon would the next mega-earthquake occur in Japan? *Nat Sci* 5(8A1):1–7. doi:10.4236/ns.2013.58A1001
- Lyubushin AA (2014) Dynamic estimate of seismic danger based on multifractal properties of low-frequency seismic noise. *Nat Hazards* 70(1):471–483
- Lyubushin AA, Kaláb Z, Lednická M (2012) Geomechanical time series and its singularity spectrum analysis. *Acta Geodaet Geophys Hung* 47(1):69–77
- Lyubushin AA, Kaláb Z, Lednická M, Haggag HM (2013) Discrimination of earthquakes and explosions using multifractal singularity spectrums properties. *J Seismol* 17(3):975–983
- Lyubushin AA, Kaláb Z, Lednická M (2014) Statistical properties of seismic noise measured in underground spaces during seismic swarm. *Acta Geodaetica Geophysica* 49(2):209–224
- Mallat S (1998) *A wavelet tour of signal processing*. Academic, San Diego, p 577
- McNamara DE, Buland RP (2004) Ambient noise levels in the continental United States. *Bull Seismol Soc Am* 94:1517–1527
- Nicolis G, Prigogine I (1989) *Exploring complexity, an introduction*. W.H. Freedman and Co., New York
- Nishida K, Kawakatsu H, Fukao Y, Obara K (2008) Background love and Rayleigh waves simultaneously generated at the Pacific Ocean floors. *Geophys Res Lett* 35:L16307
- Nishida K, Montagner J, Kawakatsu H (2009) Global surface wave tomography using seismic hum. *Science* 326(5949):112
- Poli P, Campillo M, Pedersen H, the Lapnet Working Group (2012) Body wave imaging of the Earth's mantle discontinuities from ambient seismic noise. *Science* 338:1063–1065
- Ramirez-Rojas A, Munoz-Diosdado A, Pavia-Miller CG, Angulo-Brown F (2004) Spectral and multifractal study of electroseismic time series associated to the Mw=6.5 earthquake of 24 October 1993 in Mexico. *Nat Hazards Earth Syst Sci* 4:703–709
- Rao CR (1965) *Linear statistical inference and its applications*. (Wiley, London
- Rhie J, Romanowicz B (2004) Excitation of Earth's continuous free oscillations by atmosphere-ocean-seafloor coupling. *Nature* 431:552–554
- Rhie J, Romanowicz B (2006) A study of the relation between ocean storms and the Earth's hum. *Geochem Geophys Geosyst*, Electron J Earth Sci, Volume 7, Number 10
- Schimmel M, Stutzmann E, Arduin F, Gallart J (2011) Polarized Earth's ambient microseismic noise. *Geochem Geophys Geosyst* 12:Q07014
- Shapiro NM, Campillo M, Stehly L, Ritzwoller MH (2005) High resolution surface wave tomography from ambient seismic noise. *Science* 307:1615–1618
- Shapiro NM, Ritzwoller MH, Bensen GD (2006) Source location of the 26 s microseism from cross correlations of ambient seismic noise. *Geophys Res Lett* 33:L18310
- Stehly L, Campillo M, Shapiro NM (2006) A study of the seismic noise from its long-range correlation properties. *J Geophys Res* 111:B10306
- Tanimoto T (2001) Continuous free oscillations: atmosphere-solid earth coupling. *Annu Rev Earth Planet Sci* 29:563–84
- Tanimoto T (2005) The oceanic excitation hypothesis for the continuous oscillations of the earth. *Geophys J Int* 160:276–288
- Taqqu MS (1988) Self-similar processes. *Encyclopedia of statistical sciences*, vol 8. Wiley, New York, pp 352–357
- Telesca L, Colangelo G, Lapenna V (2005) Multifractal variability in geoelectrical signals and correlations with seismicity: a study case in southern Italy. *Nat Hazards Earth Syst Sci* 5:673–677
- Yang Y, Ritzwoller MH (2008) Characteristics of ambient seismic noise as a source for surface wave tomography. *Geochem Geophys Geosyst* 9:Q02008
- Zhang J, Gerstoft P, Shearer PM (2009) High-frequency P-wave seismic noise driven by ocean winds. *Geophys Res Lett* 36:L09302
- Zhang J, Gerstoft P, Shearer P (2010a) Resolving P-wave traveltimes anomalies using seismic array observations of oceanic storms. *Earth Planet Sci Lett* 292:419–427
- Zhang J, Gerstoft P, Bromirski PD (2010b) Pelagic and coastal sources of P-wave microseisms: generation under tropical cyclones. *Geophys Res Lett* 37:L15301